Ion processing of ices and the origin of SO_2 and O_3 on the icy surfaces of the icy jovian satellites

P. Boduch[a], R. Brunetto[b], J.J. Ding[a], A. Domaracka[a], Z. Kaňuchová[c], M. E. Palumbo[d], H. Rothard[a], G. Strazzulla[d]

[a] *Centre de Recherche sur les Ions, les Matériaux et la Photonique (CEA/CNRS/ENSICAEN/UCN), CIMAP - CIRIL - GANIL, Boulevard Henri Becquerel, BP 5133, F-14070 Caen Cedex 05, France*

[b] *Institut d'Astrophysique Spatiale, CNRS, UMR-8617, Université Paris-Sud, bâtiment 121, F-91405 Orsay Cedex, France*

[c] *Astronomical Institute of Slovak Academy of Sciences, SK-059 60 Tatranská Lomnica, Slovakia*

[d] *INAF - Osservatorio Astrofisico di Catania, Via Santa Sofia 78, I-95123 Catania, Italy*

Abstract

We present new experimental results relative to 144 keV S^{9+} or Ar^{9+} ion implantation in targets made of oxygen rich frozen gases (O_2, CO_2) and mixtures with water ice. Spectra in the UV (200-400 nm) range have been obtained before and after implantation. The targets have been selected because they can be representative of the parent molecules from which SO_2 and O_3, observed to be present on the surfaces of Jupiter's icy moons, could be formed due to radiolysis induced by the abundant magnetospheric ions.

The results indicate that sulfur dioxide is not detectable after sulfur implantation in oxygen bearing species. Ozone is formed after argon and sulfur ion implantation. Sulfur implantation in O_2 and CO_2 targets also induces the formation of a band centered at about 255 nm (**that we tentatively** attribute to SO_3^- radicals). In the mixtures with water the band appears initially at the same wavelength and shifts to about 247 nm at higher ion

fluences possibly indicating the formation of sulfite (HSO_3^-) ions. An absorption band observed on Ganymede is well fitted by using three components: ozone, sulfite ions and a not identified component having an absorption band centered at 298 nm.
In all of the studied cases ion implantation produces a spectral reddening over the investigated spectral range (200-400 nm) that well mimics the observed spectral slopes of Jupiter's icy satellites.

Keywords: Jupiter, satellites, Ices, UV spectroscopy

1. Introduction

The surfaces of the icy satellites of the giant planets in the outer Solar System are dominated by water ice as deduced from many observations conducted in the visible and near IR spectral range that also evidence the presence of abundant hydrated materials (particularly sulfuric acid) and minor amounts of some volatile molecules such as H_2O_2, SO_2, and CO_2 (Carlson et al., 1997, 1999a; Carlson, 2001; Noll et al., 1995a, 1997a; Dalton et al., 2013).

Of relevance here are also observations in the UV range (200-320 nm) from which it was possible to reveal the presence of three distinct features on the surface of some of the icy satellites. These features are attributed to ozone (O_3) through the observation of its absorption band at 260 nm (Noll et al., 1996, 1997b), sulfur dioxide (SO_2) from the 280 nm band (Lane et al., 1981; Noll et al., 1997a) and a spectral reddening (relative lowering of albedo at lower wavelengths) in the observed UV range, which was attributed to poly-

meric sulfur (Carlson et al., 1999b).

Since the first detections a debate is still open on the origin and evolution of the detected species. In particular CO_2 and/or SO_2 could be formed on icy surfaces via implantation of carbon or sulfur ions present in the Jovian magnetosphere (for a review see Strazzulla, 2011). Consequently, several implantation experiments have been conducted using multiply charged carbon and sulfur ions. Results on C^{n+} (n=1, 2, 3) implantation into water ice have shown that carbon dioxide is efficiently formed by carbon ion implantation into water ice on the Galilean moons, but this is not the dominant formation mechanism (Lv et al., 2012; Strazzulla et al., 2003). It has then been suggested that the dominant mechanism is the efficient formation of CO_2 after irradiation of water ice deposited on top of carbonaceous materials. The latter is continuously delivered by impact of cometary debris on the icy moons (Mennella et al., 2004; Gomis and Strazzulla, 2005; Raut et al., 2012). **By using the fluxes given by Madey et al. (2002) it** has also been noticed that the lifetime of a carbon grain (or a layer) having a thickness of about 10 micrometers is τ=2.2$\times 10^3$ years for a grain on the surface of Europa and τ=0.7 years on Dione. The calculated lifetimes demonstrate that the solid carbon can easily dissipate by conversion into CO_2 and CO and become finally available for further radiolysis-induced processing (Sabri et al., 2015).

In addition there is a general consensus that the surface **bombardment by** the abundant energetic or plasma ions and electrons from the planetary magnetospheres drives the evolution of many surface properties. Among these properties there are the structure of the ice (amorphous vs crystalline), the ejection (sputtering) of molecular, atomic and ionized species into the ex-

osphere, and the chemical composition of the surface. As an example, on the basis of many laboratory experiments (Carlson et al., 1999a; Moore and Hudson, 2000; Gomis et al., 2004; Loeffler et al., 2006; Zheng et al., 2006), the formation mechanism of H_2O_2 is believed to be radiolysis of water ice.
Implantation of sulfur ions in oxygen bearing species has been invoked to be responsible for the formation of sulfur dioxide (Lane et al., 1981; Noll et al., 1997a) although implantation experiments and the use of IR spectroscopy have not confirmed such an hypothesis (Strazzulla et al., 2007; Ding et al., 2013).
Unfortunately, there is a scarce number of previous laboratory experiments that use UV-Vis spectroscopy to investigate the effects of energetic processing of frozen gases. In fact, most of the previous experiments have been analyzed by spectroscopy in the 1-20 μm spectral region. It has to be pointed out that many observations on planetary ices have been collected within the UV spectral region and therefore it is obvious the need for more laboratory data in that spectral region (Hendrix et al., 2013). Among the few existing experimental studies in the UV spectral region there are those in which different ions were implanted in thick water ice layers (Sack et al., 1992). These experiments led to the suggestion that the lower reflectivity of Europa's trailing hemisphere at around 280 nm can be attributed to the effect of any penetrating ion and not to SO_2 produced by either the implantation of sulfur ions from Jupiter's magnetosphere or by the preferential condensation of SO_2 from cryovolcanism (Sack et al., 1992). The UV-Vis reflectance spectrum of polymer-like sulfur residues obtained after photolysis and radiolysis of sulfur-bearing species (Strazzulla et al., 1993) well reproduces Europa's observed

reflectance spectrum (Carlson et al., 1999b). More recently new experiments have been performed on the production of ozone after 100 keV proton (Teolis et al., 2006) or 5 keV electron bombardment (Jones et al., 2014). Ozone was efficiently produced but the comparison with an UV spectrum of Ganymede (Noll et al., 1996) indicates that although ozone is present, it cannot explain the whole feature observed on that moon as an additional peak is clearly observed in the shoulder of the ozone absorption.

This paper gives a contribution to the field presenting new experimental results relative to UV (200-400 nm) spectroscopy of selected targets (the list of the experiments is given in Table 1) whose spectra have been studied before and after implantation of 144 keV S^{9+} and Ar^{9+} ions. The present targets can be representative of the parent molecules from which the observed species (namely SO_2 and O_3) could be formed after ion-induced radiolysis by the bombarding ions.

2. Experiments

Ion beams have been produced in a 14.5 GHz electron cyclotron resonance (ECR) ion source at the low energy facility ARIBE of GANIL in Caen (France). For the present experiments we used S^{9+} and Ar^{9+} ion beams with fluxes of $10^{11}-10^{12}$ ions cm^{-2} s^{-1}. Ions have been accelerated by a 16 kV/q voltage thus acquiring an energy of 144 keV. Ion beams were scanned to assure a uniform irradiation of the target. The flux of impinging projectile ions was measured and controlled during the irradiation by means of a collimator current. Before and after irradiation, a Faraday cup was inserted along the

beam line in order to measure the beam current of projectiles arriving at the target and the ratio of Faraday cup to collimator current. For more details see Lv et al. (2012).

The ice layers were prepared by condensing pure gases or their mixtures on a quartz window at 16 or 80 K. Given quantities of each molecule were introduced in a pre-chamber to obtain a gas mixture in the chosen ratio. The deposition rate was controlled by a fine valve and a nozzle was used to transmit the gas in the high vacuum chamber whose base pressure was below 10^{-7} mbar. The quartz window was installed in the center of the chamber on a cold finger connected to a closed cycle helium cryostat. The temperature of the substrate was controlled by a carbon resistance and a compound linear thermal sensor (CLTS) situated on the holder, providing a precision of 0.1 K. The cold head with the quartz window could be rotated from 0° to 180° and fixed in three positions allowing ion irradiation (0°), UV-Vis analysis (90°) and gas deposition (180°).

A Varian-Cary300 UV-Vis Spectrometer (200-800 nm) was used to analyze the sample with a spectral resolution of 0.2 nm. The spectra were taken in transmittance at normal incidence and were corrected by a background recorded before deposition.

The thickness of the sample estimated by previous calibration experiments was always in the range 1-2 μm, i.e. much larger than the penetration depth of 144 keV sulfur or argon ions in the used targets (about 0.3 μm). Ions were then implanted in the target.

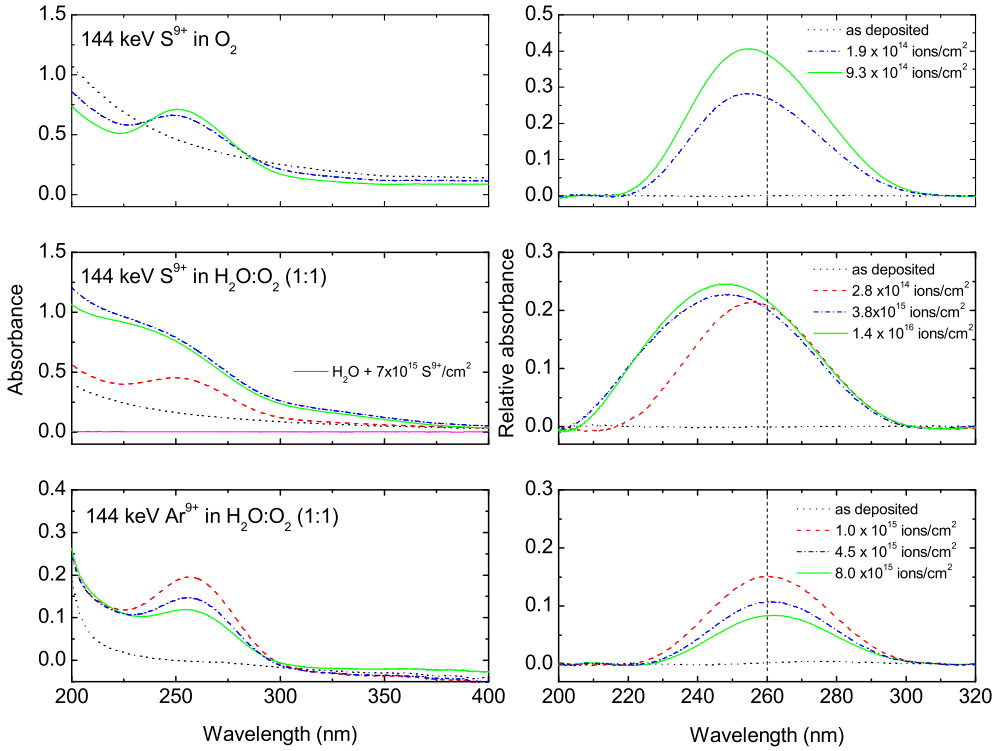

Figure 1: The left panels show the UV absorbance spectra (200-400 nm) measured before and after implantation of 144 keV S^{9+} or Ar^{9+} ions in frozen O_2, and H_2O:O_2 (1:1) gases deposited at 16 K. In the left middle panel a spectrum of pure water ice (80 K) after sulfur ion implantation is also shown for comparison. The same spectra after the continuum subtraction are shown in the right panels. The vertical line gives the position of the band of O_3 formed after photolysis of frozen oxygen.

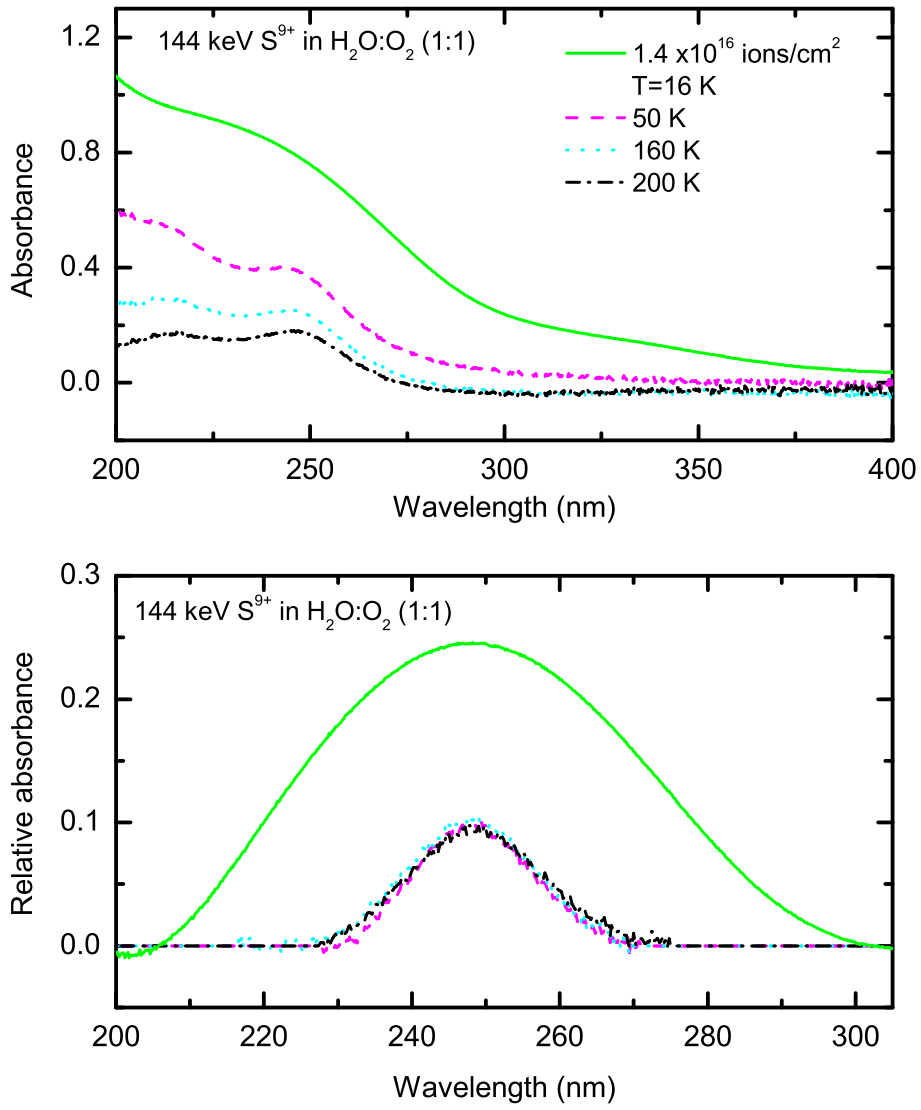

Figure 2: The top panel shows the UV absorbance spectra (200-400 nm) of H_2O:O_2 (1:1) frozen mixture implanted with 144 keV S^{9+} ions at 16 K and during the warm-up of the mixture. The spectra at T=50 K, 160 K and 200 K are scaled by a factor of 10 for a better comparison.

Table 1: List of the performed experiments. The energy of incoming ions was 144 keV.

Target	T (K)	Projectile
H_2O	80	S^{9+}
O_2	16	S^{9+}
H_2O:O_2 (1:1)	16	S^{9+}
H_2O:O_2 (1:1)	16	Ar^{9+}
CO_2	16	S^{9+}
H_2O:CO_2(1 : 1)	16	S^{9+}
SO_2	80	not irradiated

3. Results

The left panels of Fig. 1 show the UV absorbance spectra (200-400 nm) measured before and after implantation of 144 keV S^{9+} or Ar^{9+} in frozen O_2, H_2O, and H_2O:O_2 (1:1) gases deposited at 16 or 80 K. The projectile ion fluences range from 10^{14} to 10^{16} ions/cm^2. The absorbance of all samples presented in Fig. 1 (except pure water) exhibits an initial slope due to the continuum absorption of the oxygen molecule, in particular due to the so called Rydberg continuum (Cooper et al., 2003) and to a possible contribution due to scattering because of surface roughness. In all of the considered cases, **except H_2O**, an absorption band appears when the sample is irradiated. When the continuum is subtracted (right panels of Fig. 1), it comes evident that the peak position is significantly different for the two different projectiles (see the detailed discussion in Section 4). The vertical lines in the panels indicate the position of the ozone band (260 nm) as measured after UV photolysis of solid molecular oxygen (our unpublished data). We can see that the band produced after Ar implantation is peaked at the same wavelength and can easily be attributed to ozone formation. The band formed after sulfur implantation exhibits a position that ranges from 255 to 247 nm as

the number of implanted ions increases (see also Fig. 5). As also discussed in Section 4, we **tentatively** interpret this as due to the formation of (SO_3^-) radical and sulfite (HSO_3^-) ions that exhibit significant absorptions in that spectral region when soluted in water (Hayon et al., 1972).

In the middle panel on the left side of Fig. 1 a spectrum of pure water ice after sulfur ion implantation is shown: no ozone is detectable. This is in agreement with the finding from previous experiments (Teolis et al., 2006; Strazzulla, 2011). Also evident is a general increase of the slope of the spectrum (except in the case of pure oxygen that as deposited shows a strong continuum absorption that decreases upon irradiation). Slopes and band area variations will be discussed in detail later (Section 4).

After irradiation the samples were heated. The spectra for the H_2O:O_2 sample irradiated with 1.4×10^{16} S^{9+} ions/cm^2 acquired at increasing temperatures as shown in Fig. 2. The band formed after the subtraction of the continuum is shown in the bottom panel. From the top panel we see that after warming up the spectrum is not flat. This is due to presence of a thin layer (1-10 monolayers) made of a left over refractory sulfur **residue** exhibiting two bands at 220 and 249 nm. The band at 249 nm is quite similar in peak position and shape to the one formed at low temperature.

As listed in Table 1, further experiments have been done on CO_2 bearing frozen gases. The left panels in Fig. 3 show the UV absorbance spectra (200-400 nm) measured before and after implantation of 144 keV S^{9+} in frozen CO_2, and H_2O:CO_2 (1:1) gases deposited at 16 K. Also for these experiments projectile fluences range from 10^{14} to 10^{16} ions/cm^2. We can see that an absorption band appears that is even more evident, after continuum

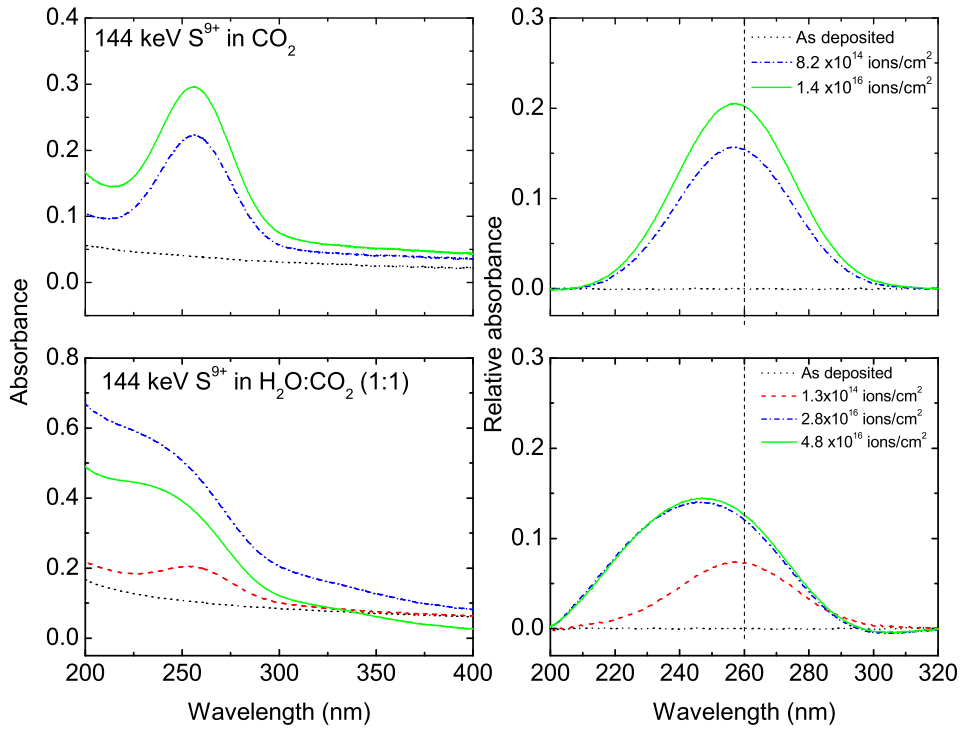

Figure 3: The left panels show the UV absorbance spectra (200-400 nm) measured before and after implantation of 144 keV S^{9+} ions in frozen CO_2, and H_2O:CO_2 (1:1) gases deposited at 16 K. The same spectra after the continuum subtraction are shown in the right panels.

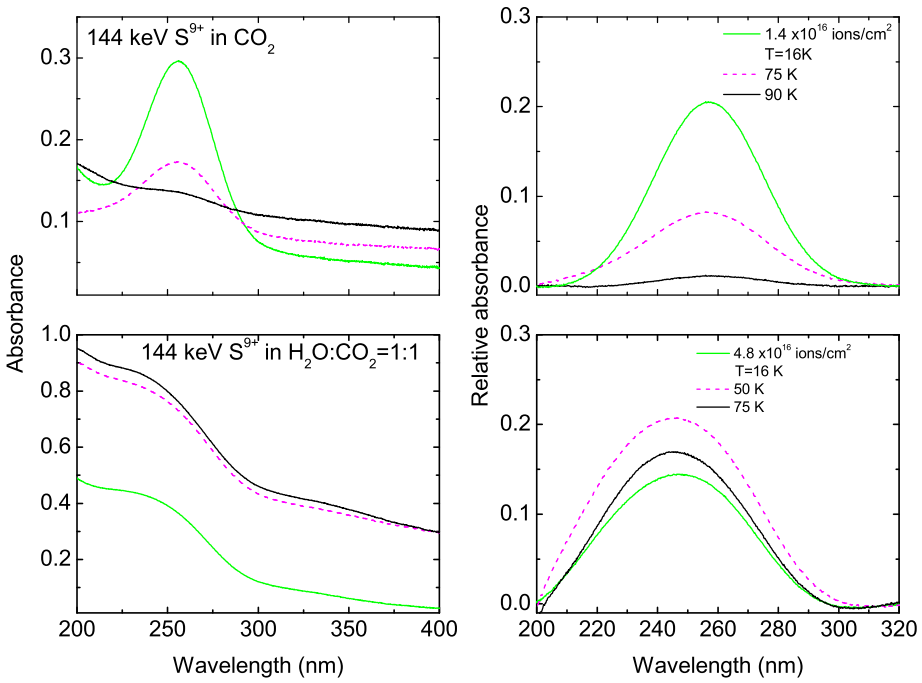

Figure 4: The left panels show the UV absorbance spectra (200-400 nm) measured during the warm up of in frozen CO_2, and H_2O:CO_2 (1:1) gases implanted with 144 keV S^{9+} ions at 16 K. The same spectra after the continuum subtraction are shown in the right panels.

removal, in the right panels of Fig. 3. The vertical lines in the right panels indicate the position of the ozone band (260 nm): in the case of pure CO_2 the peak position remains constant (255 nm). **We tentatively attribute this to** the formation of SO_3^- radicals; in the case of the mixture it varies with the increasing projectile fluence probably due to the formation of sulfite ions. Also evident is the slope increase with ion fluence, particularly in the case of the mixture.

After irradiation the samples were heated and the spectra acquired at increasing temperatures are shown in Fig. 4, compared with the spectra obtained after the last irradiation at low temperature. We can see that the peak position does not change during the warm up for the H_2O:CO_2 sample irradiated with 1.4×10^{16} S^{9+} ions/cm^2. In the left panel the spectra are the "as acquired" ones, in the right panel the band formed is shown after the subtraction of the continuum. Also in this case a thin layer made of a refractory sulfur **residue** is left over at room temperature. **The increase of the intensity of the band in the mixture upon warm up (50 K) is not uncommon and is due to an increase in the relative band strength. At higher temperatures the intensity of the band decreases because CO_2 begins to segregate (75 K) and then to sublimate (90 K) and left over the thin residue.**

4. Discussion

The experimental results reported in this paper are summarized in Fig. 5 where the band areas (top panels; nm), the band slopes (middle panels, nm^{-1}) and the peak position (bottom panels; nm) are reported as a function

of the ion fluence. "Band area" refers to the area of the band in the 200-300 nm region formed upon ion implantation in oxygen or carbon dioxide rich ices. In the middle panels the horizontal lines represent the interval of the band slopes measured in some regions of Europa (Hendrix and Johnson, 2009). Also Ganymede and Callisto exhibit "red spectra" in that spectral range (Hendrix and Johnson, 2008a) which in some cases are larger than those of Europa.

The band slopes have been quantified by:

$$BS = \frac{Abs_{\lambda 2} - Abs_{\lambda 1}}{\Delta\lambda} \quad (1)$$

$\lambda 1$ and $\lambda 2$ being the limits of the band (the exact value changes by few nm), $\mathrm{Abs}_{\lambda 2}$ and $\mathrm{Abs}_{\lambda 1}$ the absorption values at $\lambda 1$ and $\lambda 2$ and $\Delta\lambda$ is the difference $\lambda 2$-$\lambda 1$.

Although it is not straightforward to compare the absolute values of the slopes measured in the laboratory with those measured on the icy moons, we can safely say that the laboratory measurements indicate a general increase in the absolute value of the spectral slope and a decrease in the albedo with increasing ion fluences comparable to what is observed in the remote sensing observations of Europa.

The results relative to the band peak position (bottom panels in Fig. 5) give important clues on the origin of the band. There is no question that the band formed after Ar implantation in oxygen bearing targets is peaked at about 260 nm and it is attributable to ozone (see also Teolis et al., 2006). Sulfur implantation in the same targets produces a band with a peak position at about 255 nm that in the case of the mixture with water decreases

to 247 nm as the number of implanted ions increases. The same behavior is observed when CO_2 replaces O_2. The peak positions in the region around 250 nm are typical of the SO_3^- radical and sulfite (HSO_3^-) ions diluted in water (Hayon et al., 1972). Consequently we interpret our results as due to the initial formation of SO_3^- radicals. The availability of hydrogen in mixtures with water allows the formation of sulfite ions at higher S-implantation fluences. **Such attributions are however only tentative and it would be necessary to study the spectra of the radical and ionic species in ice rather than in liquid water. At present we have not been able to do that. In addition, it would be interesting to evaluate the relative contributions to the observed band of ozone and that of the sulfur bearing species. At present this is however not possible mainly because the band strengths of the two components that depend, as known, on many parameters (e.g. temperature, mixture, structure of the ice) are not known.**

It is important to note that the time scales corresponding to the ion fluences reported in Fig. 5 are short. In fact the fluxes of sulfur (keV-MeV) ions in selected regions of the surface of Europa have been evaluated to vary between about 2×10^6 to 10^8 ions cm^{-2} s^{-1} (Dalton et al., 2013). Thus the time necessary to accumulate a fluence of 10^{16} S-ions cm^{-2} is of the order of 3-150 years.

One of the purposes of this paper was to investigate the formation of SO_2 present on icy satellites for which several mechanisms have been proposed. As said the presence of sulfur dioxide has been proved via the observation of the band at 280 nm as shown in Fig. 6 where the band observed on a region

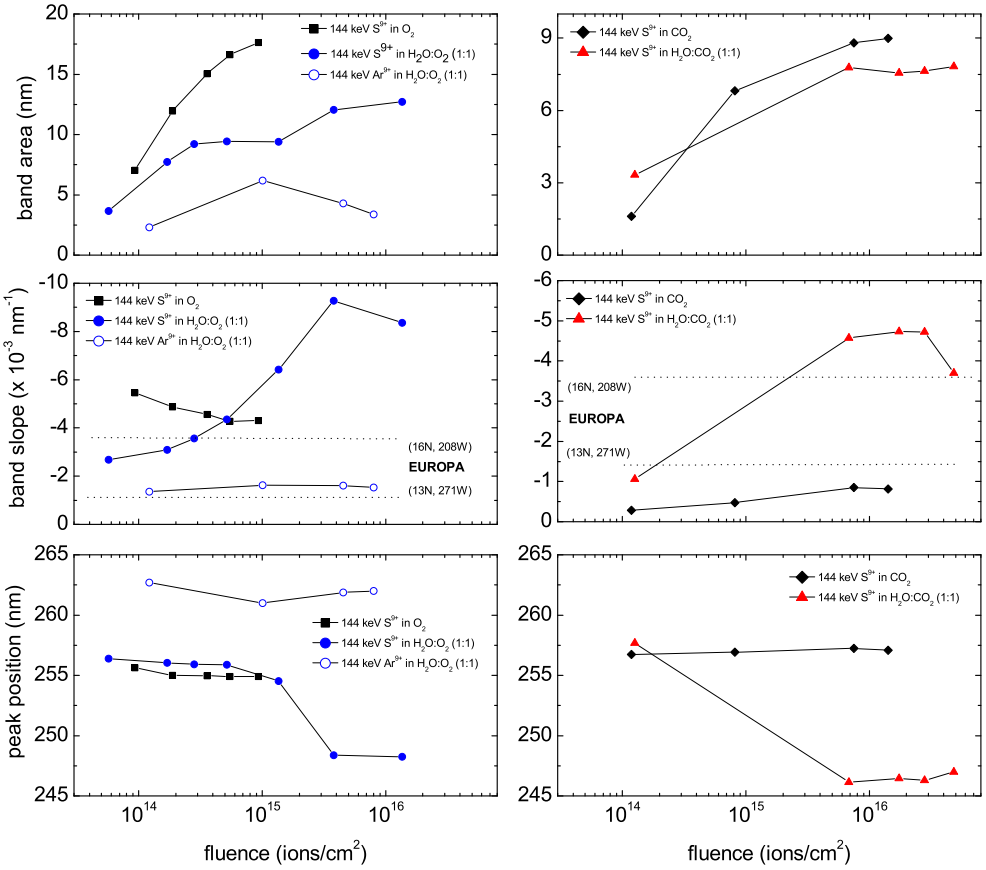

Figure 5: Top panels: area (nm); middle panels: band slopes (see eq. 1); bottom panels: peak position of the band formed upon ion implantation in oxygen or carbon dioxide rich ices. In the middle panels the band slope interval measured in two representative regions of Europa are also reported.

of Europa (Hendrix and Johnson, 2009) is compared with a spectrum of solid sulfur dioxide measured in the laboratory at 80 K (see Table 1). Please note that the scaling is quite arbitrary and it only implies that the observed feature is coincident with laboratory spectra of frozen sulfur dioxide. The suggested formation mechanisms include S implantation (Lane et al., 1981; Sack et al., 1992), volcanism (Sack et al., 1992), an endogenic source (Noll et al., 1995b), and synthesis from a radiolytic cycling of sulfur (Carlson et al., 1999b). **In the case of Callisto, SO_2 being detected on the leading hemisphere which is less exposed to ion bombardment, an endogenic source seems to be favored (Noll et al., 1997a). Such a conclusion has been disputed (Hendrix and Johnson, 2008b) and, in addition, an exogenic source by sulfur ion implantation has also been suggested (Lane and Domingue, 1997)**.

Recently, the full set of high-resolution observations from the Galileo Ultraviolet Spectrometer (UVS) was analyzed to look for spectral trends across the surface of Europa: Hendrix et al. (2011) provided the first disk-resolved map of the 280 nm SO_2 absorption feature. They also investigated its relationship with sulfur and electron flux distributions and with other surface features, namely UV albedo (300-310 nm). The large-scale pattern of sulfur dioxide absorption band is similar to the pattern of sulfur ion implantation, but with strong variations in band depth depending on the terrain. In particular, the young chaos units show stronger SO_2 absorption bands than expected from the average pattern of sulfur ion flux. Hendrix et al. (2011) suggested this is due to a local source of SO_2, or diapiric heating that leads to a sulfur-rich lag deposit. The relation with the UV albedo is even more

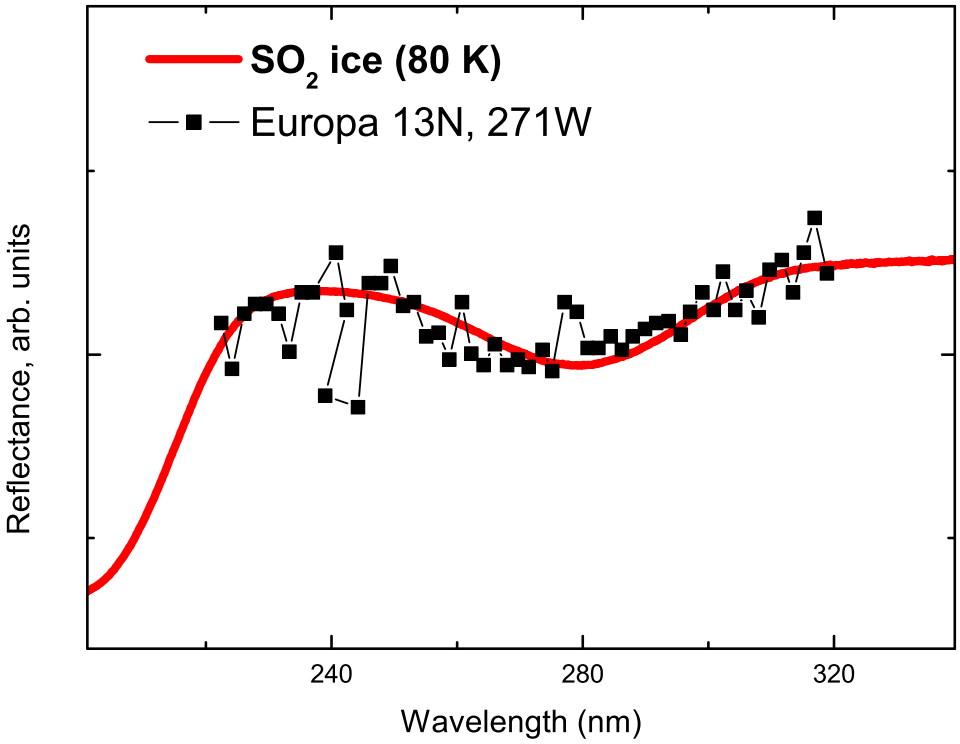

Figure 6: Comparison of a UV spectrum observed on a region of Europa (Hendrix and Johnson, 2009) with a spectrum of solid sulfur dioxide measured in the laboratory.

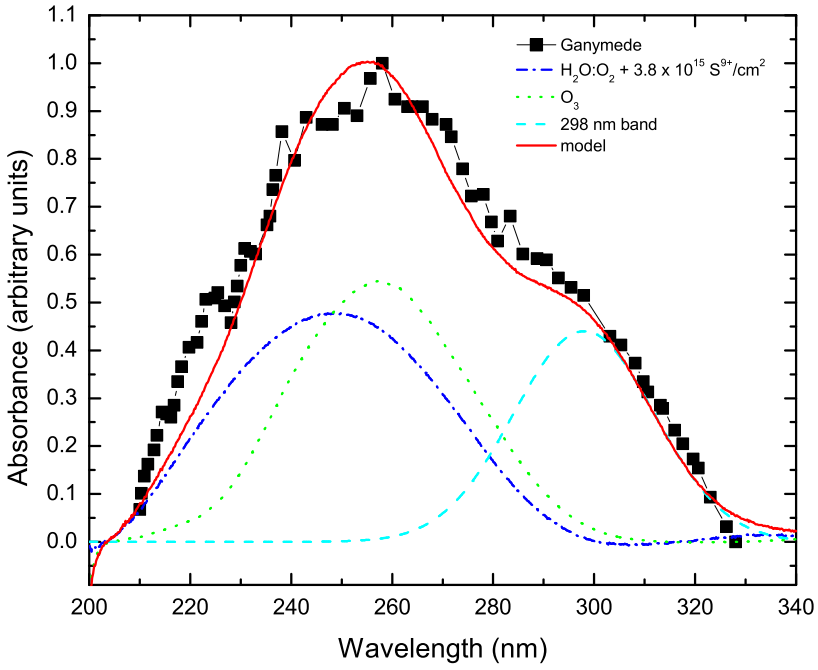

Figure 7: The absorption band observed on Ganymede (Noll et al., 1996) is fitted by using three components as indicated in the figure (see details in the text).

complex: the SO_2 feature is confined to the trailing hemisphere, the near UV albedo has a global pattern with a minimum at the center of the trailing hemisphere and a maximum at the center of the leading hemisphere. Hendrix et al. (2011) suggested that the global nature of the albedo pattern is indicative of an exogenic source while, as said, the SO_2 absorption also has local variations that depend on terrain type and age.

The results presented in this paper confirm those conclusions: there are no spectral evidences of the appearance of UV features attributable to sul-

fur dioxide after sulfur implantation. In fact some SO_2 was expected to be formed after S-implantation in pure carbon dioxide as evidenced by a previous study conducted by IR spectroscopy (Lv et al., 2014). However, the formation yield was measured to be about 0.38 SO_2 molecules formed per impinging ion. The maximum fluence in the present experiments was 1.4×10^{16} S-ions cm^{-2} that would produce about 5×10^{15} SO_2 molecules cm^{-2} that is below the detection limit of the present experiments. Moreover it overlaps with the very intense band related to the formation of SO_3^- or HSO_3^-. Experiments have been also performed with water ice layers deposited on top of sulfurous solid materials to see if sulfur dioxide molecules can be formed at the interface, similarly to what was observed for CO_2 formed at the interface ice/carbonaceous solids (Gomis and Strazzulla, 2005). The results were negative: sulfur dioxide is not formed in detectable quantity (Gomis and Strazzulla, 2008). We therefore support the hypothesis that sulfur dioxide observed at the surface of Europa, and possibly the other icy moons, is the result of endogenic processes. However, once exposed at the surface it is progressively destroyed by ion bombardment that mostly produces SO_3 polymers as demonstrated by many previous experiments (see e.g. Moore et al., 2007; Gomis and Strazzulla, 2008). At the same time ion bombardment produces an increase of the absorbance (albedo decrease) in the whole UV region with a spectral reddening as demonstrated by the present experiments.

It seems more simple to explain the surface distribution of sulfuric acid. There is in fact a clear correlation between sulfur ion flux and the concentration of sulfuric acid hydrates (Dalton et al., 2013). This finding coupled with the high formation yields of hydrated sulfuric acid measured in the labora-

tory after sulfur ion implantation (Strazzulla et al., 2007; Ding et al., 2013) strongly supports an exogenic origin of sulfur.

As already mentioned a band centered at about 260 nm has been observed to be present on the surface of some icy moons, in particular Ganymede (Noll et al., 1996). **Noll et al. (1996) ratioed the disk-integrated trailing hemisphere albedo to the disk-integrated leading hemisphere albedo and attributed the observed feature to the presence of ozone. Hendrix et al. (1999) presented observations of disk-resolved albedos of Ganymede that because of the procedure followed, results in a different band shape that the authors define as "ozone-like". The feature observed by Noll et al. (1996) is reported in Fig. 7.** We have attempted to fit the data points by using the spectra obtained in the experiments reported here. The obtained best fit is shown in the same Fig. 7. To fit the observed feature we had to use three components: the first is ozone obtained by photolysis of solid molecular oxygen (our unpublished spectrum) which is quite similar to that obtained after implantation of Ar ions (such a component accounts for 37% of the observed feature), the second is the spectrum obtained after implantation of sulfur ions in oxygen rich mixtures that we attribute to SO_3^- radicals and sulfite (HSO_3^-) ions (accounts for 40%), and a third band that is a gaussian centered at 298 nm (accounts for 23%). Of course, these relative contributions of the three components to the observed band area do not imply that they correspond to the abundance of the relative species. We are not able to do any quantitative estimation because it would be necessary to know the optical constants of the components and use an appropriate model. Our fit

only implies the need of, at least, three components.

The need for an additional component longward the ozone band was already outlined by Teolis et al. (2006) and Jones et al. (2014). Here, we suggest that an additional component is present at the shorter wavelengths and we suggest this is probably due to the presence of sulfur bearing species. We have searched for plausible compounds having absorption close to the wavelength of the 298 nm component. Among the candidates there are $Al_2Si_2O_5(OH)_4$ kaolinite (Babin and Stramski, 2004) and NO_3^- nitrate ions (Maria et al., 1973; Karlsson et al., 1995). The latter, however, has a much stronger band at 190 nm.

5. Conclusion

It is well known that ion implantation of magnetospheric ion populations into the surfaces of icy moons in the outer Solar System is a relevant, often dominant, mechanism to drive the physico-chemical properties of the irradiated ices. This statement is supported by a plethora of laboratory experiments that, however, have mostly investigated the induced effects by using Vis-IR spectroscopy. Nevertheless very relevant astronomical observations have been obtained in the UV range (200-320 nm) for which there are only few laboratory experiments. This paper contributes to fill the gap by presenting new experimental results relative to UV spectroscopy of selected targets made of oxygen rich frozen ices (O_2, CO_2) and mixtures with water ice (see Table 1) irradiated with 144 keV S^{9+} or Ar^{9+} ions.

The present results confirm that sulfur dioxide is not detectable after sulfur

implantation in oxygen bearing species. As demonstrated by the detection of an absorption band at 260 nm, ozone is easily formed after argon and sulfur ion implantation. Sulfur implantation also induces the formation of a band centered at about 255 nm in O_2 and CO_2 targets. In the mixtures with water, the band appears initially at the same wavelength and shifts to about 247 nm at higher ion fluences. This band is **tentatively** attributed to the formation of SO_3^- radicals for the single ice targets and to sulfite (HSO_3^-) ions for the mixtures. We have also shown that the absorption band observed on Ganymede is well fitted by using three components: ozone, sulfite ions and a not identified component having an absorption band centered at 298 nm.

In all of the studied cases ion implantation produces a spectral reddening over the investigated spectral range (200-400 nm) that well mimics the observed spectral slopes of Jupiter's icy satellites.

Acknowledgement

We thank T. Been, F. Noury and J. M. Ramillon for their technical assistance. This work was also supported by COST Action TD 1308. Z.K. was supported by VEGA - The Slovak Agency for Science, Grant No. 2 / 0032 / 14. G.S. was supported by University Paris Sud and Italian Space Agency (ASI 2013-056 JUICE Partecipazione Italiana alla fase A/B1).

6. References

Babin, M., Stramski, D.. Variations in the mass-specic absorption coefficient of mineral particles suspended in water. Limnol Oceanogr 2004;49:756 – 767.

Carlson, R.W.. Spatial distribution of carbon dioxide, hydrogen peroxide, and sulfuric acid on Europa. In: Division for Planetary Sciences Meeting Abstracts. volume 33; 2001. p. 1125.

Carlson, R.W., Anderson, M.S., Johnson, R.E., Smythe, W.D., Hendrix, A.R., Barth, C.A., Soderblom, L.A., Hansen, G.B., McCord, T.B., Dalton, J.B., et al. Hydrogen peroxide on the surface of Europa. Science 1999a;283(5410):2062–2064.

Carlson, R.W., Johnson, R.E., Anderson, M.S.. Sulfuric acid on Europa and the radiolytic sulfur cycle. Science 1999b;286:97–99. doi:10.1126/science.286.5437.97.

Carlson, R.W., Smythe, W.D., Lopes-Gautier, R.M.C., Davies, A.G., Kamp, L.W., Mosher, J.A., Soderblom, L.A., Leader, F.E., Mehlman,

R., Clark, R.N., Fanale, F.P.. Distribution of sulfur dioxide and other infrared absorbers on the surface of Io. Geophys Res Lett 1997;24:2479. doi:10.1029/97GL02609.

Cooper, P.D., Johnson, R.E., Quickenden, T.I.. A review of possible optical absorption features of oxygen molecules in the icy surfaces of outer solar system bodies. Planet Space Sci 2003;51:183–192. doi:10.1016/S0032-0633(02)00205-2.

Dalton, J.B., Cassidy, T., Paranicas, C., Shirley, J.H., Prockter, L.M., Kamp, L.W.. Exogenic controls on sulfuric acid hydrate production at the surface of Europa. Planet Space Sci 2013;77:45–63. doi:10.1016/j.pss.2012.05.013.

Ding, J.J., Boduch, P., Domaracka, A., Guillous, S., Langlinay, T., Lv, X.Y., Palumbo, M.E., Rothard, H., Strazzulla, G.. Implantation of multiply charged sulfur ions in water ice. Icarus 2013;226:860–864. doi:10.1016/j.icarus.2013.07.002.

Gomis, O., Leto, G., Strazzulla, G.. Hydrogen peroxide production by ion irradiation of thin water ice films. A&A 2004;420:405–410. doi:10.1051/0004-6361:20041091.

Gomis, O., Strazzulla, G.. CO_2production by ion irradiation of H_2O ice on top of carbonaceous materials and its relevance to the Galilean satellites. Icarus 2005;177:570–576.

Gomis, O., Strazzulla, G.. Ion irradiation of H_2O ice on top of sulfurous solid residues and its relevance to the Galilean satellites. Icarus 2008;194:146–152. doi:10.1016/j.icarus.2007.09.015.

Hayon, E., Treinin, A., Will, J.. Electronic Spectra, Photochemistry, and Autoxidation Mechanism of the Sulfite-Bisulfite-Pyrosulfite Systems. The SO,-, SO,-, SO,-, and SO,- Radicals . J Am Chem Soc 1972;94:47–57. doi:10.1021/ja00756a009.

Hendrix, A.R., Barth, C.A., Hord, C.W.. Ganymede's ozone-like absorber: Observations by the Galileo ultraviolet spectrometer. JGR 1999;104:14169–14178. doi:10.1029/1999JE900001.

Hendrix, A.R., Cassidy, T.A., Johnson, R.E., Paranicas, C., Carlson, R.W.. Europa's disk-resolved ultraviolet spectra: Relationships with plasma flux and surface terrains. Icarus 2011;212:736–743. doi:10.1016/j.icarus.2011.01.023.

Hendrix, A.R., Domingue, D.L., Noll, K.S.. Ultraviolet Properties of Planetary Ices. p. 73. doi:10.1007/978-1-4614-3076-6_3.

Hendrix, A.R., Johnson, R.E.. Callisto and Ganymede: New Results from the Galileo UVS. In: Lunar and Planetary Science Conference. volume 39 of *Lunar and Planetary Inst. Technical Report*; 2008a. p. 2035.

Hendrix, A.R., Johnson, R.E.. Callisto: New Insights from Galileo Disk-resolved UV Measurements. ApJ 2008b;687:706–713. doi:10.1086/591491.

Hendrix, A.R., Johnson, R.E.. Europa: A New Look at Galileo UVS Data. In: Lunar and Planetary Science Conference. volume 40 of *Lunar and Planetary Inst. Technical Report*; 2009. .

Jones, B.M., Kaiser, R.I., Strazzulla, G.. UV-Vis, Infrared, and Mass Spectroscopy of Electron Irradiated Frozen Oxygen and Carbon Dioxide Mixtures with Water. ApJ 2014;781:85. doi:10.1088/0004-637X/781/2/85.

Karlsson, M., Karlberg, B., Olsson, R.J.O.. Determination of nitrate in municipal waste water by UV spectroscopy . Analytica Chimica Acta 1995;312:107 – 113.

Lane, A.L., Domingue, D.L.. IUE's View of Callisto: Detection of an SO2 Absorption Correlated to Possible Torus Neutral Wind Alterations. GRL 1997;24:1143. doi:10.1029/97GL00884.

Lane, A.L., Nelson, R.M., Matson, D.L.. Evidence for sulphur implantation in Europa's UV absorption band. Nat 1981;292:38. doi:10.1038/292038a0.

Loeffler, M.J., Raut, U., Vidal, R.A., Baragiola, R.A., Carlson, R.W.. Synthesis of hydrogen peroxide in water ice by ion irradiation. Icarus 2006;180:265–273. doi:10.1016/j.icarus.2005.08.001.

Lv, X.Y., Boduch, P., Ding, J.J., Domaracka, A., Langlinay, T., Palumbo, M.E., Rothard, H., Strazzulla, G.. Sulfur implantation in CO and CO_2 ices. MNRAS 2014;438:922–929. doi:10.1093/mnras/stt2004.

Lv, X.Y., de Barros, A.L.F., Boduch, P., Bordalo, V., da Silveira, E.F., Domaracka, A., Fulvio, D., Hunniford, C.A., Langlinay, T., Mason,

N.J., McCullough, R.W., Palumbo, M.E., Pilling, S., Rothard, H., Strazzulla, G.. Implantation of multiply charged carbon ions in water ice. A&A 2012;546:A81. doi:10.1051/0004-6361/201219886.

Madey, T.E., Johnson, R.E., Orlando, T.M.. Far-out surface science: radiation-induced surface processes in the solar system. Surface Science 2002;500:838–858. doi:10.1016/S0039-6028(01)01556-4.

Maria, H.J., McDonald, J.R., McGlynn, S.P.. Electronic Absorption Spectrum of Nitrate Ion and Boron Trihalides . Journal ofthe Americun Chemical Society 1973;95:1050 – 1056.

Mennella, V., Palumbo, M.E., Baratta, G.A.. Formation of CO and CO_2 molecules by ion irradiation of water ice-covered hydrogenated carbon grains. APJ 2004;615:1073.

Moore, M.H., Hudson, R.L.. IR Detection of H_2O_2 at 80 K in Ion-Irradiated Laboratory Ices Relevant to Europa. Icarus 2000;145:282–288. doi:10.1006/icar.1999.6325.

Moore, M.H., Hudson, R.L., Carlson, R.W.. The radiolysis of SO_2 and H_2S in water ice: Implications for the icy jovian satellites. Icarus 2007;189:409–423. doi:10.1016/j.icarus.2007.01.018.

Noll, K.S., Johnson, R.E., Lane, A.L., Domingue, D.L., Weaver, H.A.. Detection of Ozone on Ganymede. Science 1996;273:341–343. doi:10.1126/science.273.5273.341.

Noll, K.S., Johnson, R.E., McGrath, M.A., Caldwell, J.J.. Detection of SO_2 on Callisto with the Hubble Space Telescope. Geophys Res Lett 1997a;24:1139–1142.

Noll, K.S., Roush, T.L., Cruikshank, D.P., Johnson, R.E., Pendleton, Y.J.. Detection of ozone on Saturn's satellites RHEA and Dione. Nature 1997b;388:45–47. doi:10.1038/40348.

Noll, K.S., Weaver, H.A., Gonnella, A.M.. The albedo spectrum of Europa from 2200 Å to 3300 Å. J Geophys Res 1995a;100:19057–19059.

Noll, K.S., Weaver, H.A., Gonnella, A.M.. The albedo spectrum of Europa from 2200 Å to 3300 Å. JGR 1995b;100:19057–19060. doi:10.1029/94JE03294.

Raut, U., Fulvio, D., Loeffler, M.J., Baragiola, R.A.. Radiation Synthesis of Carbon Dioxide in Ice-coated Carbon: Implications for Interstellar Grains and Icy Moons. ApJ 2012;752:159. doi:10.1088/0004-637X/752/2/159.

Sabri, T., Baratta, G.A., Jäger, C., Palumbo, M.E., Henning, T., Strazzulla, G., Wendler, E.. A laboratory study of ion-induced erosion of ice-covered carbon grains. A&A 2015;575:A76. doi:10.1051/0004-6361/201425154.

Sack, N.J., Johnson, R.E., Boring, J.W., Baragiola, R.A.. The effect of magnetospheric ion bombardment on the reflectance of Europa's surface. Icarus 1992;100:534–540. doi:10.1016/0019-1035(92)90116-O.

Strazzulla, G.. Cosmic ion bombardment of the icy moons of Jupiter. Nucl Instrum Meth B 2011;269:842–851.

Strazzulla, G., Baratta, G.A., Leto, G., Gomis, O.. Hydrate sulfuric acid after sulfur implantation in water ice. Icarus 2007;192:623–628.

Strazzulla, G., Leto, G., Gomis, O., Satorre, M.A.. Implantation of carbon and nitrogen ions in water ice. Icarus 2003;164:163–169.

Strazzulla, G., Leto, G., Palumbo, M.E.. Ion irradiation experiments. Advances in Space Research 1993;13:189–198. doi:10.1016/0273-1177(93)90069-N.

Teolis, B.D., Loeffler, M.J., Raut, U., Famá, M., Baragiola, R.A.. Ozone Synthesis on the Icy Satellites. ApJL 2006;644:L141–L144. doi:10.1086/505743.

Zheng, W., Jewitt, D., Kaiser, R.I.. Temperature Dependence of the Formation of Hydrogen, Oxygen, and Hydrogen Peroxide in Electron-Irradiated Crystalline Water Ice. ApJ 2006;648:753–761. doi:10.1086/505901.